

Visual Inspection of Cylindrical Product's Lateral Surface using Cameras and Image Processing

Mohammed A.H. Ali, M. Mailah, H.H. Tang and S. Kazi

Abstract—Visual inspection using cameras is used here for testing the lateral surface of cylindrical products. The inspection can be carried out according to available resources by: line scan camera system, matrix camera with conical mirror system and matrix camera with multi flat mirrors system. The research is aimed to use the previous systems for testing the objects surface and making comparison between the mentioned systems. This requires suitable setting of each system to perform experiments and getting images, includes: setting of camera, light, object and mirrors. The image of each system has a different view from each other and it is quite difficult to make directly comparison between them. For this reason, the images should have the same view for its lateral surface, so called the developed view. The image of the line scan camera is used as a reference for the developed view and the images coming from matrix camera with conical mirror and multi flat mirrors are manipulated using image processing in MATLAB program to find the developed view of lateral surface of the inspected object. The developed view of the images from the previous systems is compared in terms of their resolution and accuracy, for the same tested object, in order to choose which system is suitable for the inspection task.

Keywords— Conical mirrors, image processing in MATLAB, line scan camera, matrix camera, multiple flat mirrors.

I. INTRODUCTION

THE finishing surface of industrial parts such as shafts, bearings, pistons, rings and pins should be smooth within the permissible limits before installation process, as the defects in these parts may damage or reduce the life of machine.

There are several inspections methods that can be divided into two groups: Destructive inspection methods (DT), Nondestructive testing (NDT), depending on the required degree of surface smoothness and the presence of defects in crystalline structure of these parts.

Visual test is one of the famous methods of non destructive tests. It gives the possibility to detect the defects like: shape defects, corrosions, fatigue cracks and leaks at different stages during the production process, which eventually results in time-savings and lower financial costs.

Manuscript received January 3, 2012.

All authors are with the Department of System Dynamics and Control, Faculty of Mechanical Engineering, Universiti Teknologi Malaysia, 81310 UTM Johor Bahru, Johor MALAYSIA.

E-mails(moh-ali-hashim@maktoob.com, musa@fkm.utm.my, tanghh@fkm.utm.my, skazi75@gmail.com)

This test can be carried out either by naked eye inspections (not applicable and inaccurate), or by inspections with the use of endoscope, magnifying glass and cameras.

Several researches have been done in the area of automatic visual inspection for testing the surface objects which can be from simple surface like sheets to complex like cylindrical, multi-shape objects. Zhang *et al.* presented an automatic vision system to detect and classify surface defects due to the processes of grinding and polishing [1]. Omar *et al.* has provided a system capable of self-adjustment painting booth operation for an automotive fuel tank production, based on the defects detected by automatic inspection system [2]. Jia *et al.* proposed a real-time visual inspection system that uses vector machine to automatically learn complex defect patterns [3]. Norifumi *et al.* innovated a new method based on an optics model for highly reliable surface inspection of industrial parts [4]. Sun *et al.* proposed a real-time imaging and detection system for weld defects in steel tubes [5]. Rosati *et al.* presented an automatic defects detection for coated plastic component in automotive industry [6]. Laurowski *et al.* and Demoynek *et al.* have proposed 3D objects inspection systems that can be used for path planning and localizing these products during machining operations [7, 8, 9].

In this research, line scan and matrix camera system were used to visually inspect the lateral surface of cylindrical object against surface defects.

Line scans camera system gives the opportunity to perform image acquisition of cylindrical object's surface line by line, while matrix camera system is well suited for text recognition and image processing in one-frame unit. Two systems are designed to inspect the cylindrical objects using matrix camera:

- Camera with conical mirror.
- Camera with multiple flat mirrors.

The images from the cameras should be manipulated by image processing programs in order to either improve its pictorial information for human interpretation or for autonomous machine perception [10]. The processing of images in this project has been done using special codes in MATLAB, which stores images as matrices, in order to make these images suitable for utilizing in comparison step between the three systems with a condition that ensure good extracting of features.

II. LINES SCAN CAMERA SYSTEM

A line scan camera is an image capturing device having a CCD sensor which is formed by a single line of photosensitive elements (pixels). The line scan camera should be used in applications where high resolution images are required, and for inspecting the objects which moves like sheet (continuous processing).

The hardware of this system as illustrated in Fig. 1, consists of the following parts:

- 1- Line scan camera with lens: DALSA S2-11-05H40, base camera link with 8 bit with CCD 512 pixels, C-Mount.
- 2- Holder of camera which maintains the camera in the correct position of object.
- 3- Holder of object with capability of rotation using stepper motor.
- 4- Holder of light to produce homogeneous light.

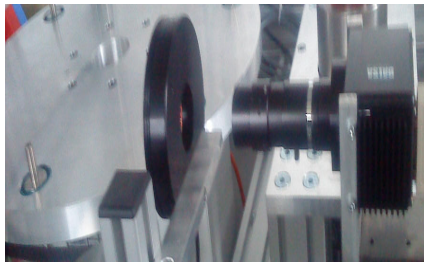


Fig. 1: Line scan camera system

A number of experiments have been done considering different cylindrical objects with varying heights and diameters. The setting of the experiment for the line scan camera was as follows: The distance between the lens and the inspected object is 200 mm and the distance between the light source and the inspected object is 150 mm. The lens used is TAMRON with magnification 1:3.9, diameter of the lens, $\text{Ø}=25.5$ mm, focal length=75mm. The image for the object is shown in Fig. 2a while Fig. 2b depicts the image by using the line scan camera system.

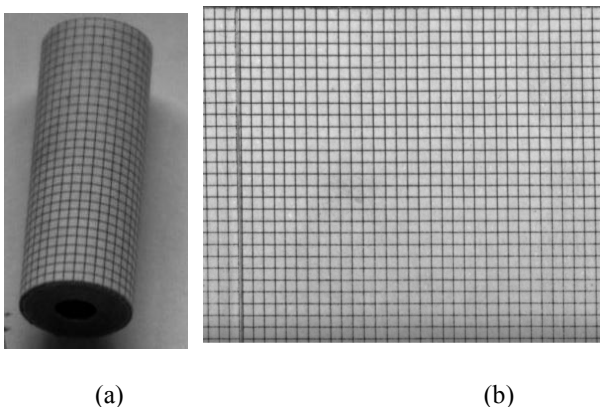


Fig. 2: (a) Horizontal and vertical lines pattern on cylindrical object ($D=11$ mm, $H=30$ mm). (b) Image acquired of this object by line scan camera.

III. MATRIX CAMERA SYSTEM

Matrix camera is an array image sensor, which uses a rectangular mosaic of pixels to capture an image. This camera works well to capture the large objects smaller than the field-of-view of a camera. Two experimental setups for performing this inspection system are employed, namely, the matrix camera system with conical mirror system and matrix camera system with multiple flat mirrors system as explained in the following sections.

A. Matrix Camera System with Conical Mirror System

The hardware components of this system as shown in Fig. 3a include the following parts:-

- 1- Matrix camera: the camera used for this purpose is JAI CV-M1 with (1300×1030) pixels CCD sensor, C-Mount.
- 2- Conical mirror: the angle of this cone is 45° , diameter of bottom base is 11mm.
- 3- Base body.
- 4- Holder of mirror.
- 5- Holders of camera.
- 6- Holders of object.
- 7- Holders of light



(a)



(b)

Fig. 3: (a) Matrix camera with conical mirror system. (b) Close view of conical mirror.

The image of the object in Fig. 2a is shown in Fig. 4 through matrix camera with conical mirror.

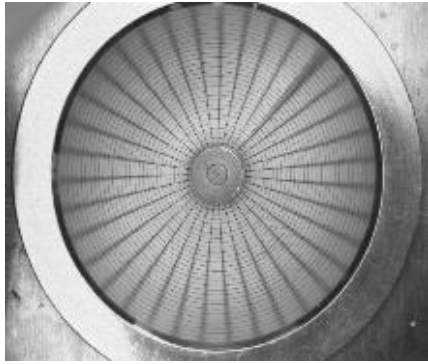


Fig. 4: Image of cylindrical object in matrix camera with conical mirror system.

B. Matrix Camera System with Multiple Flat Mirrors System

The multiple flat mirrors system as shown in Fig. 5a consists of the following parts:-

- 1- Matrix camera: the camera is JAI CV-M1 with (1300×1030) pixels CCD sensor, C-Mount.
- 2- Multiple flat mirrors: five mirrors (50mm×20mm×3mm) supported by holders on the ring using taped glue as in Fig. 5b.
- 3- Ring with 16 division angle: A range with outer radius=167mm and inner radius=120mm with thickness 15mm) gives us a possibility to divide the range into sixteen sectors (each one can hold mirror).
- 4- Connection beams: five beams (80mm×20mm×8mm) connect the holder of mirrors to ring.
- 5- Mirror holders it has incidence of 45°.
- 6- Object holder: cylindrical part with 50 mm in diameter and with 200mm in height is supported in the exact middle of range.
- 7- Base body. 8- Holders of cameras. 9- Holders of light.



(a)



(b)

Fig. 5: Matrix camera with multiple flat mirrors system. (b) Close view of multi flat mirrors.

The image resulted from setting in Fig. 2a is shown in Fig. 6.

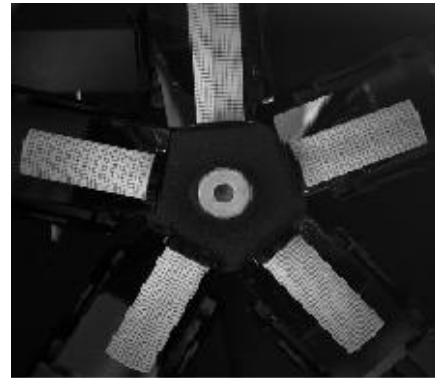


Fig. 6: Image of cylindrical object in matrix camera with multiple flat mirrors system.

IV. DEVELOPED VIEW OF MATRIX CAMERA'S IMAGES

In order to compare the previous inspection systems, to decide which one is suitable for this project, there is a need to make a graphic model with similar development view of the three systems, which produce the cylindrical object in a rectangular shape, since this view is able to produce enormous information for defects of objects, as shown in Fig. 2b. This is due to the fact that the images taken from these systems cannot be compared directly, as shown in Figs. 2b, 4 and 6. The images of the cylindrical object in line scan camera are used as reference as shown in Fig. 2b and the images from matrix camera are processed in MATLAB to find the rectangular developed view.

A. Developed View of Matrix Camera with Conical Mirror

The images from the matrix camera with conical systems have to be processed through two steps, in order to extract the developed rectangular view:

1) *Mathematical model*: The cylindrical object can be described in cylindrical coordinate system as shown in Fig. 7.

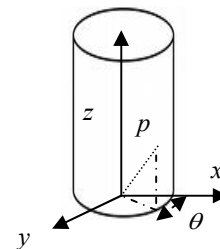


Fig. 7: Cylindrical object coordinate system.

From Fig. 7, any point p in the lateral surface of object has in cylindrical coordinate system the following dimensions as in Eqs. 1-3:

$$x = r \cos \theta \quad (1)$$

$$y = r \sin \theta \quad (2)$$

$$z = z \quad (3)$$

Where θ is the angle between the original coordinate system and the choosing point. r is the radius of the object and it has constant value. z is the height of this points in the direction of z starting from 0 to h height of the object.

This lateral circumference surface of the object occurs in the camera's image like a disk shape as shown in Fig. 8.

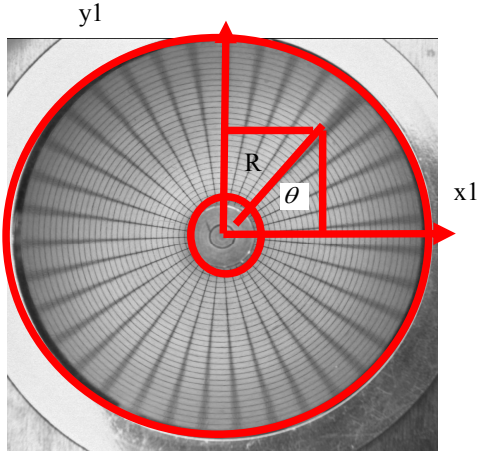


Fig. 8: Camera's image of cylindrical object in the image coordinate system.

Any points in the previous disk can be described in the image coordinate system x_1, y_1 as depicted in Fig. 8 by Eqs. 4 and 5 as follows:

$$x_1 = R \cos \theta \tag{4}$$

$$y_1 = R \sin \theta \tag{5}$$

Where R is the radius of the disk starting from the inner radius of disk to the outer radius of disk.

Note: The inner radius of the disk in the image = radius of the object, taking into consideration the effect of the lens.

The value of R in the image coordinate system can be found using r and z from the cylindrical object coordinate system taking into consideration the magnification effect of the lens and the type of camera used. This effect is called the factor of lens and camera fc . R can be calculated from Eq. 6 as follows:

$$R = fc (z \tan \alpha + r) \tag{6}$$

Where α is the conical mirror angle.

If the value of R from Eq. 4,5 is compensated in Eq. 6, one gets Eq. 7,8:

$$x_1 = fc (z \tan \alpha + r) \cos \theta \tag{7}$$

$$y_1 = fc (z \tan \alpha + r) \sin \theta \tag{8}$$

In order to get the lateral circumference surface of the cylindrical object as the image of line scan camera view, the disk view coming from image coordinate system is developed

to a rectangle view. The intermediate step is to transfer every circular line in the disk into horizontal straight line. The factor used for transferring the circular sector line (as shown in Fig

9a) to a straight line is $2\pi R \frac{\theta}{360}$ (Fig. 9.b). Then the straight

lines in Fig. 9b are stretched using the factor, $\frac{(h \tan \alpha + r)}{(z \tan \alpha + r)}$, in order to make the bottom surface of the object looks like the upper surface as shown in Fig. 9c.

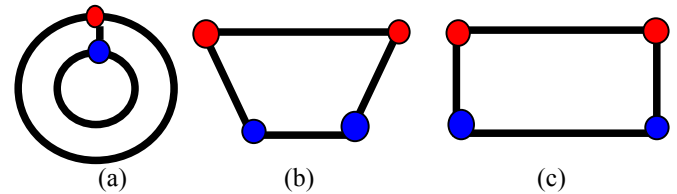


Fig. 9: Steps for transferring image's view of object (a) to developed view (c).

At the end, the developed view of the whole lateral surface can be described in Cartesian coordinate system, x_2, y_2 as shown in Fig. 10.

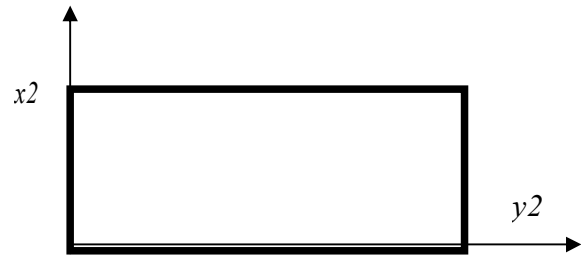


Fig. 10: Developed view of the lateral surface of object

Any point of the developed view of this object can be described in Cartesian coordinate system of the developed view x_2 and y_2 as illustrated in Eqs. 9 and 10.

$$y_2 = 2\pi fc (z \tan \alpha) \frac{\theta}{360} \frac{(h \tan (\alpha + r))}{(z \tan (\alpha + r))} \tag{9}$$

$$x_2 = fc z \tan \alpha \tag{10}$$

Any point in the coordinate system of the cylindrical object x, y, z can be transferred to the image coordinate system x_1, y_1 and the developed view coordinate system x_2, y_2 , and vice versa.

2) *MATLAB Algorithm:* The MATLAB algorithm consists of the following steps:

- Reading and cropping the image with the dimensions described in Eq. 11:

$$x = y = 2(br) \tag{11}$$

Where, (br) is the largest circular line, as shown in Fig. 4.

- Transferring of the symmetrical rotating lines to normal straight lines: The lateral surface of the inspected cylindrical object is shown in Fig. 4 as circular lines. The equation of the

circle generates positive and negative values, and unfortunately, the MATLAB image processing program can deal only with positive values. Therefore, the circle is divided into four sections as described in Eqs. 12-15 as follows:

First quarter: $(Sx-x)^2 + (Sy-y)^2 = r^2$ (12)

Second quarter: $(x-Sx)^2 + (Sy-y)^2 = r^2$ (13)

Third quarter: $(x-Sx)^2 + (y-Sy)^2 = r^2$ (14)

Fourth quarter: $(Sx-x)^2 + (y-Sy)^2 = r^2$ (15)

Where, (Sx, Sy) is the center of the circle (known).

From the above equations, and in order to find the value of third variable, the value of the two variables should be known. Also, in order to increase the accuracy and avoid squared highest values, every quarter is divided into two sections as shown in Fig. 11.

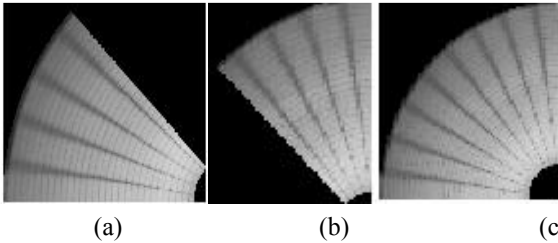


Fig. 11: Combining the left half (a) and right half (b) to get the first quarter (c).

Then, every circular line has to be transferred to a normal line by using special assignment code in MATLAB as shown in Fig. 12.

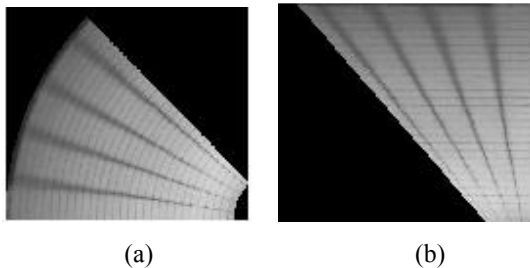


Fig. 12: Transferring step of circular lines into straight lines.

In the previous step, the outcome of the straight lines as shown in Fig. 12b have no similar length, so a measuring scale algorithm is used. If the length of the lines from the biggest radius is br and from the smallest radius sr , the measuring scale is as expressed in Eq. 16 as follows:

$$ms = br / (br - sr + 1) \tag{16}$$

The result is illustrated in Fig. 13.

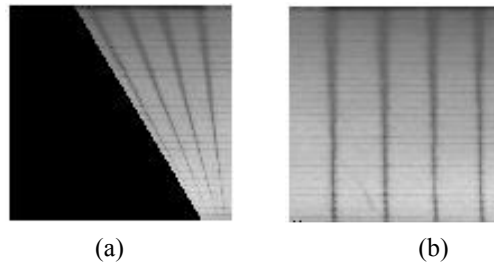


Fig. 13: Stretch of lines from (a) to (b) done by MATLAB program.

- Filtration: As the values of the pixel's coordinate system must be always be an integer in MATLAB, the approximating values should be derived from Eqs. 12-16. Two dimensional order statistic filters were used for this purpose as shown in Fig. 14.

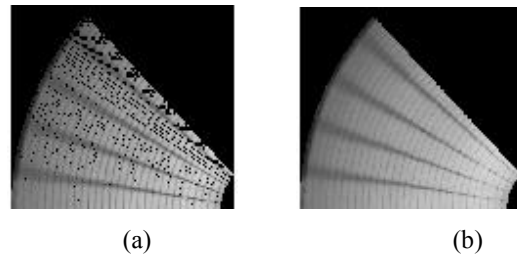


Fig. 14: The effects of Two Dimensional Order filter (a) Image before filter (b) Image after filter.

The two sections of these quarters must be reflected, as shown in Fig. 15.

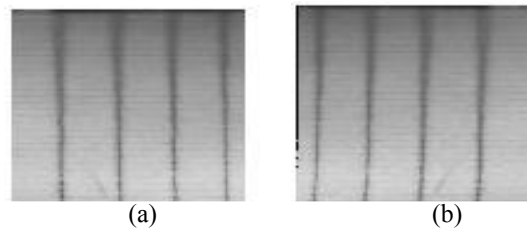


Fig. 15: (a) Half section of the quarter need to reflect (b) Reflection of this section.

The collections of the quarters in one frame are the developed view of the matrix camera with conical mirror as shown in Fig. 16.

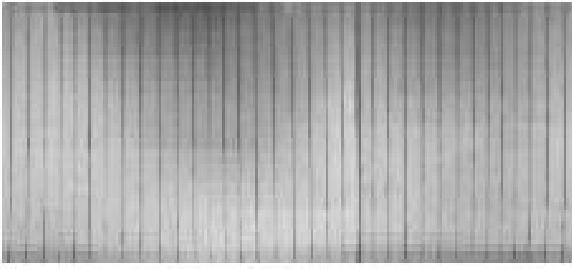


Fig. 16: Developed view of the object in matrix camera with conical mirror.

B. Developed View of the Matrix Camera with Multiple Flat Mirrors

The images from the matrix camera with five flat mirrors systems have to be manipulated through two steps, in order to extract the developed rectangular view:

1) *Mathematical model:* The previous cylindrical object as depicted in Fig. 7 can be inspected using five flat mirrors with one camera system.

Any point on the circumference of the cylindrical object can be described in a coordinate system, the so called real coordinate system xrf, yrf and zrf as expressed in Eqs. 17-19.

$$xrf = r \cos \theta \tag{17}$$

$$yrf = r \sin \theta \tag{18}$$

$$zrf = z \tag{19}$$

Where θ changes from 0 to 360°. r is the radius of the object and it has constant value. z is the height of the object and it changes from 0 at the bottom base of cylindrical object to h which is the top part of the cylindrical object.

The object and the setting of the partial mirror are described in global coordinate system by five partial coordinate system as shown in Fig. 17:

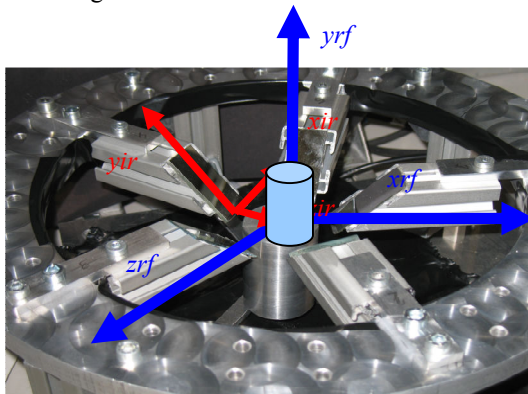


Fig. 17: Global coordinate system and partial coordinate system in multi flat mirrors

The angle between the axes xrf, yrf of the global coordinate system and the partial coordinate $(x_i r, y_i r)$ is explained as follows: For first mirror, the angle is ψ_1 , the second mirror, $\psi_2 = \psi_1 + 72^\circ$, the third mirror $\psi_3 = \psi_1 + 144^\circ$, fourth mirror

$\psi_4 = \psi_1 + 216^\circ$ and fifth mirror $\psi_5 = \psi_1 + 288^\circ$. The angle between axes zrf of the global coordinate system and the partial coordinate of the partial mirrors $z_i r$ is α which is equal to 45° in this setting. The partial coordinate system can be described in relative to the global coordinate system as given in Eq. 20.

$$\begin{bmatrix} x_i r \\ y_i r \\ z_i r \end{bmatrix} = \begin{bmatrix} 0 & \cos \alpha & \sin \alpha \\ 0 & -\sin \alpha & \cos \alpha \\ 1 & 0 & 0 \end{bmatrix} \begin{bmatrix} \cos \psi_i & \sin \psi_i & 0 \\ -\sin \psi_i & \cos \psi_i & 0 \\ 0 & 0 & 1 \end{bmatrix} \begin{bmatrix} xrf \\ yrf \\ zrf \end{bmatrix} \tag{20}$$

The partial axes $(x_i r, y_i r)$ describe the view of the object in the mirrors, where $z_i r$ describe the thickness of mirrors.

The previous description using 3D coordinate system is useful for describing the setting of the system, but it is not useful to describe image in the partial mirrors because the image has only two axes coordinate system. Therefore the coordinate system with two axes is used to find the position of every points in the image of the cylindrical object, thus it is called the image coordinate system. Each partial mirror's image can be described by special two axes coordinate system as shown in Fig. 18.

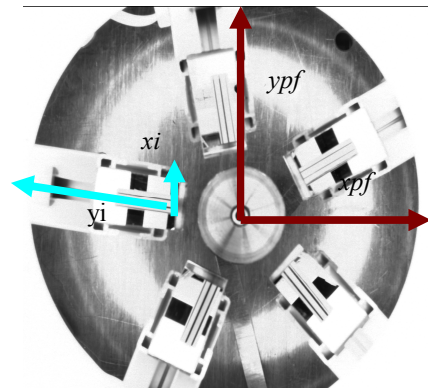


Figure 18: Coordinate system of partial mirrors and fixed image coordinate system

x_i, y_i special coordinate system for each mirror.

xpf, ypf fixed image coordinate system.

The image coordinate system applies to the real coordinate system mentioned above with a scale related to the kind of camera and lens used as described by Eqs. 21-24.

$$xpf = fc \cdot xrf \tag{21}$$

$$ypf = fc \cdot yrf \tag{22}$$

$$y_i = fc \cdot y_i r \cdot \cos \alpha \tag{23}$$

$$x_i = fc \cdot x_i r \cdot \sin \alpha \tag{24}$$

Any point in these mirrors can be described in special coordinate of each mirror as follows:

Every circular lines in object will occur as straight horizontal lines in mirrors (see Fig 19), and therefore we can find that in

the ideal case, this straight lines have the same length with the diameter of the circle, i.e., $2R$.

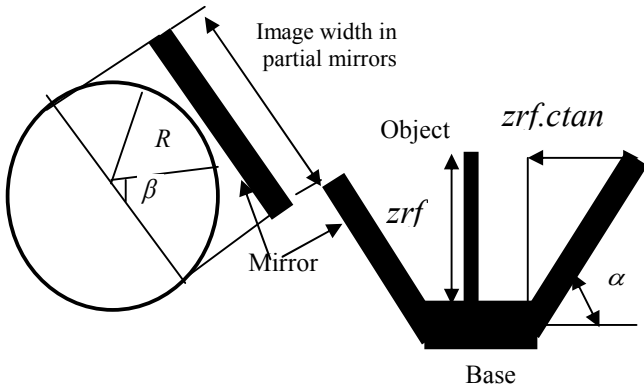


Fig. 19: (a) Image width of cross section of object in partial mirror (b) Length of object in partial mirror.

This length can be described using the special coordinate system of each mirror as given in Eq. 25.

$$xi = R \cos \beta \quad \text{and} \quad yi = fc.zrf.c \tan \alpha \quad (25)$$

Where β changes from 0 to 180° in every special coordinate system. $R = fc.r$ is the radius of the object in the image coordinate system which is greater than r (radius of the object) by a factor fc (the effect of camera and lens). α is the angle of mirrors in z direction.

It is noticed that some parts of the image occur twice and in order to capture the parts which occur only once in each mirror, the pentagon dimensions and angles should be derived as shown in Fig 20a. The required pentagon is one in which the five sides are located inside of circle as shown in Fig. 20b.

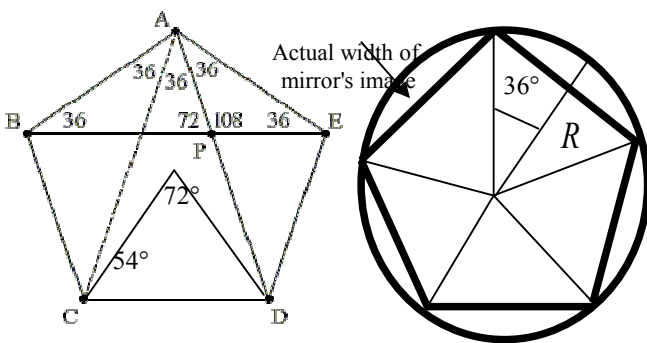


Fig. 20: (a) Geometrical properties of pentagon (b) Property of five partial mirror system

From Fig. 19, the angle β should be changed between (54° and 126°) to ensure that the width of the image in each partial mirror can occur only once, which can be calculated using Eq. 26 as follows:

$$xi = R \cos \beta \quad 54^\circ \geq \beta \geq 126^\circ \quad (26)$$

The position of any point in each mirror coordinate system can be calculated in the image coordinate system. The total angle of mirrors location in relation to the image coordinate system can be calculated using Eq. 27:

$$\varphi = \psi + \omega \quad (27)$$

Where ψ is the constant angle for each mirror described before. ω is the rotational angle of whole system about the reference image coordinate system.

The point p on the circumference of the object can be described in the image coordinate system for those parts which occur only once in each related partial mirrors as given in Eq. 28.

$$\begin{bmatrix} xpf \\ ypf \end{bmatrix} = \begin{bmatrix} \cos \varphi_i & \sin \varphi_i \\ -\sin \varphi_i & \cos \varphi_i \end{bmatrix} \begin{bmatrix} xi + ti \\ yi + gi \end{bmatrix} = \begin{bmatrix} \cos \varphi_i & \sin \varphi_i \\ -\sin \varphi_i & \cos \varphi_i \end{bmatrix} \begin{bmatrix} fc.r \cos \beta_i + ti \\ fc.zrf.c \tan \alpha + gi \end{bmatrix} \quad (28)$$

Where $\varphi_i + 36 \geq \theta \geq \varphi_i - 36$, t is the shifting of every partial mirror axes to the center of image coordinate system in x direction. g is the shifting of every partial mirror axis to the center of image coordinate system in y direction.

The five partial views of the image in mirrors are collected in one view, which looks like those shown in Fig. 21. It can be described in the so called collecting coordinate system, xcf, ycf and the relationship between xif, yif and xcf, ycf will be described by Eq. 29 as follows:

$$ycf = ypf \quad (29)$$

$$xcf = xpf + u_i \quad (30)$$

where u_i is accumulating width of the mirrors that can be calculated as follows:

$u1=0; u2=w; u3=u2+w=2w; u4=u3+w=3w; u5=u4+w=4w$, where w is the actual width of the mirror (see Fig. 20b). Eqs. 29-30 can be rewritten as described in Eq. 31 as follows:

$$\begin{bmatrix} xcf \\ ycf \end{bmatrix} = \begin{bmatrix} \cos \varphi_i & \sin \varphi_i \\ -\sin \varphi_i & \cos \varphi_i \end{bmatrix} \begin{bmatrix} xi + ti + u_i \\ yi + gi \end{bmatrix} = \begin{bmatrix} \cos \varphi_i & \sin \varphi_i \\ -\sin \varphi_i & \cos \varphi_i \end{bmatrix} \begin{bmatrix} fc.r \cos \beta_i + ti + u_i \\ fc.zrf.c \tan \alpha + gi \end{bmatrix} \quad (31)$$

Where $\varphi_i + 36 \geq \theta \geq \varphi_i - 36$

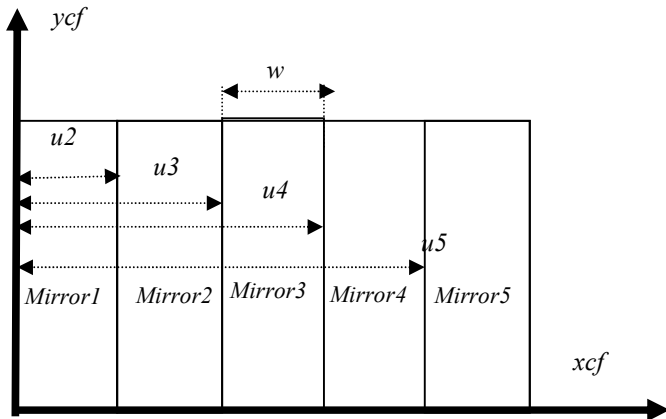


Fig. 21: Scheme of the developed view of multi flat system

The mirrors coordinate system can be described in the real object coordinate system taking into consideration the factor related to the types of cameras and lens fc . Thus, Eqs. 25-30 can be written in real coordinate system using the following transformation as described in Eq. 32.

$$\begin{bmatrix} xi + ti \\ yi + gi \end{bmatrix} = fc \cdot \begin{bmatrix} \cos \varphi_i & -\sin \varphi_i \\ \sin \varphi_i & \cos \varphi_i \end{bmatrix} \begin{bmatrix} xrf \\ yrf \end{bmatrix} \quad (32)$$

Where $\varphi_i + 36 \geq \theta \geq \varphi_i - 36$

From previous Eqs. 17-32, if any point of the object is known in real coordinate system (xrf, yrf, zrf) , it's position can be found in partial coordinate system (xi, yi) and image coordinate system (xpf, ypf) , vice versa.

2) *MATLAB Algorithm:* In order to get the image from the five partial mirrors system as shown in Fig. 5, it should be initially marked on the base, the global coordinate system (xrf, yrf, zrf) and a partial mirror coordinate system of all the mirrors (xi, yi, zi) . The camera axes should be focused at the center of the object.

The following algorithm is used for manipulating the image in this system:

- Reading, cropping and rotating image for the partial mirrors.
- Capturing the image of object in each mirror: The axes of the partial mirrors should meet each other at the center of object. Due to some deformation in the hardware system, some correction in angles of the mirrors has been done. Eq. 33 is used to capture every mirror image:

$$x_i = y_i \tan \varphi_i \pm \frac{d}{2} \quad (33)$$

Where, $\varphi_i = \psi_i + \omega_i$, ψ is a constant angle for each mirror and depending on the pentagon properties $\psi_{i+1} = \psi_i + 72^\circ$. xi and yi are the coordinate system of each mirror. ω is the rotational angle of the whole system around the reference image coordinate system, d is the diameter of the object. Due to the previous captured image from every mirror positioned at a certain angle, the program rotates this image till it is in

vertical direction and then cuts the interested captured image, as shown in Fig. 22.

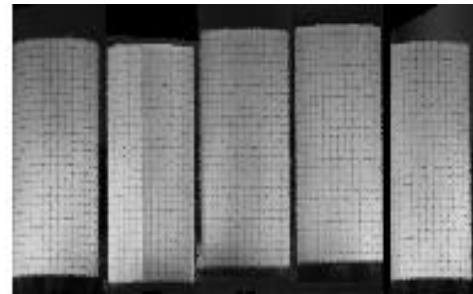


Fig. 22: The five captured partial images of object.

- Registration: Special registration has been done for the partial view of mirrors in relation to the calculation of the equal sides of pentagon with conditions that the center of tested part meets the center of mirrors axes. The capturing width of object in all mirrors is equal to the diameter of the tested part inserted by the user. The software program calculates the angles from the first mirror axes, which are incrementally increased by $(360^\circ/5= 72^\circ)$. As the mirrors are supported in ring with an angle 72° between them respectively, the difference between the hardware and software measurement is small. The actual width for each mirror is calculated depending on the property of the pentagon (with equal sides). The final registration of this tested object is illustrated in Fig. 23.

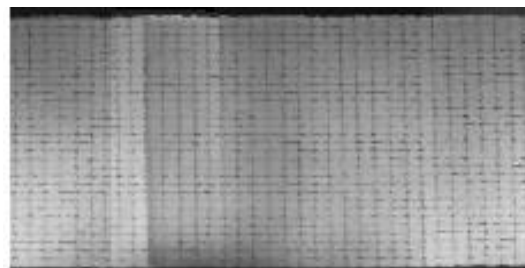


Fig. 23: Developed view of registration the partial views of mirrors using program in MATLAB.

The accuracy of the registration between the five partial mirrors is shown in Fig. 24.

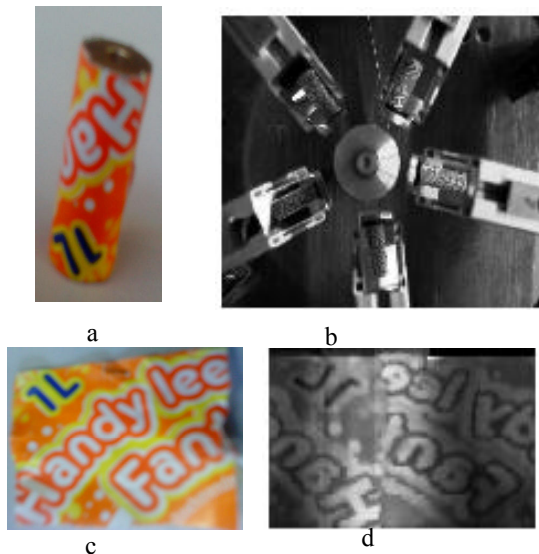


Fig. 24: (a) Pattern of letters that covered cylindrical object. (b) Image from the matrix camera with multiple flat mirrors. (c) Cover before placing on object. (d) Developed view of the partial views of mirrors after image processing.

V. COMPARISON BETWEEN INSPECTION SYSTEMS

A number of experiments have been done for inspecting the objects in these systems. The horizontal and vertical lines pattern object of Fig. 2a is illustrated via the line scan camera shown in Fig. 2b. Similarly, the developed view of the matrix camera with conical mirror and five flat mirrors are shown in Figs. 16 and 23, respectively. The image resolution of these objects is best observed in the line scan camera system in comparison to the matrix camera counterpart. The accuracy of the image with the effect of non-homogeneous lighting that is acquired by the five mirrors is relatively not as efficient as the improved conical mirrors, but the line scan camera system has the best accuracy.

VI. CONCLUSION

The line scan camera system should be used to inspect the cylindrical object with multi-diameters components as it produces high resolution images for inspected object and accurate images without distortions for some applications. On the other hand, the matrix camera should be used for faster application and it saves more power compared to the line scan camera which requires the rotation of the object, accumulating light and adjusting the camera field.

The matrix camera with conical mirror has some advantages over the multi flat mirrors system in which the former produces a full field view of the object compared to the latter system. However, the matrix camera with multi flat mirror system should be used instead of the conical mirror system to inspect the objects having different diameters. The comparison between these systems in terms of the resolution and accuracy is always significant, depending on the results of the experiments, for the same tested objects. The image produces by the line scan camera has the best accuracy and best

resolution, whereas the developed view through the use of matrix camera with conical mirror has good resolution and accuracy while that with five flat mirrors gives good resolution but bad accuracy.

REFERENCES

- [1] Zhang X, Krewet C, Kuhlenkoetter B. "Automatic classification of defects on the product surface in grinding and polishing". *International Journal of Machine Tools Manufacture*, Vol. 46, No. 1, 2006, pp 59–69.
- [2] Omar M, Viti V, Saito K, Liu J. Self-adjusting robotic painting system. *International Journal of Industrial Robot*; Vol. 33, No. 1, 2006, pp50–55.
- [3] Jia H, Murphey YL, Shi J, Chang T-S. "An intelligent real-time vision system for surface defect detection". In: *Proceedings of the 17th international conference on pattern recognition*, Cambridge, UK, August 23–26, 2004.
- [4] Norifumi K, Mutsuo S, Shuichi O, Masashi O. "A method for inspecting industrial parts surfaces based on an optics model". *Journal of Machine Vision and Applications*, Vol. 12 No. 4, 2000, pp. 170–176.
- [5] Sun Y, Bai P, Sun Hy, Zhou P. "Real-time automatic detection of weld defects in steel pipe". *NDT&E International*, Vol. 38, No. 7, 2005, pp. 522–528.
- [6] Rosati G, Boschetti G, Biondi A and Rossi A. "Real-time defect detection on highly reflective curved surfaces". *Optics and Lasers in Engineering* Vol. 47, 2009, pp. 379–384
- [7] M. Weyrich, P. Klein, M. Laurowski, Y. Wang, "Vision based Defect Detection on 3D Objects and Path Planning for Processing", *Proceedings of the 9th WSEAS International Conference on ROCOM*. 2011.
- [8] O. Demuynck, C. P. Cedeno, A. L. Moore, "Industrial Machine Vision System for Fast and Precise 3D Object Localization," in *Proceedings of the 9th WSEAS International Conference on Signal Processing, Computational Geometry and Artificial Vision*, 2009.
- [9] M. Weyrich, M. Laurowski, P. Klein, and Y. Wang. "A Real-time and Vision-based Methodology for Processing 3D Objects on a Conveyor Belt". In *WSEAS International Journal of Systems Applications, Engineering & Development* Issue 4, Vol. 5, 2011.
- [10] Gonzalez R, Woods R and Eddins S. *Digital Image Processing Using MATLAB*. Prentice Hall. 2004.
- [11] M. Ali, M. Mailah, S. Kazi and T. Hing. " Defects Detection of Cylindrical Object's Surface Using Vision System". In *Proceeding of The 10th WSEAS International Conference on Computational Intelligence, Man-Machine Systems and Cybernetics (CIMMACS '11)*, Jakarta, 1-3 December, 2011.